

# Revealing Diffusion Frequency-Dependence in Surface-to-Volume Ratio limit using OGSE sequence on the Connectome 2.0 Scanner

Jialan Zheng<sup>1,2,3</sup>, Wen Zhong<sup>1</sup>, Dongsuk Sung<sup>3,4</sup>, Julianna Gerold<sup>3</sup>, Qiyuan Tian<sup>1,5</sup>, Hua Guo<sup>1</sup>, Susie Huang<sup>3,4</sup> and Hong-Hsi Lee<sup>3,4</sup>

<sup>1</sup>School of Biomedical Engineering, Tsinghua University, Beijing, China

<sup>2</sup>Tanwei College, Tsinghua University, Beijing, China

<sup>3</sup>Athinoula A. Martinos Center for Biomedical Imaging, Massachusetts General Hospital, Charlestown, MA, USA

<sup>4</sup>Harvard Medical School, Boston, MA, USA

<sup>5</sup>Tsinghua Laboratory of Brain and Intelligence, Tsinghua University, Beijing, China

## Primary

Category: Diffusion

Subcategory: Simulation/Validation

## Secondary

Category: Diffusion

Subcategory: Microstructure

**General Keyword:** Simulation/Validation

## Synopsis (100 words)

### Motivation.

Diffusion frequency-dependence offers a direct probe to tissue microstructure at diffusion length scale. Oscillating-gradient-spin-echo (OGSE) sequence provides very short effective diffusion time and length for evaluating fine structures but poses challenges in simultaneously achieving high diffusion-weighting and high frequency on human scanners.

### Goal(s).

To validate the potential of OGSE sequences on the high-gradient-performance Connectome 2.0 scanner.

### Approach.

We measured diffusivity frequency-dependence (30-100Hz) in an anisotropic solid-fiber phantom on Connectome 2.0 and estimated surface-to-volume ratio and fiber radius, whose value was corrected for non-ideal cosine-OGSE waveform.

### Results.

Estimated fiber radius matched the ground-truth (error<5%), demonstrating the potential of in vivo microstructural imaging using OGSE.

**Impact (35 words)**

We performed diffusion frequency-dependence using oscillating-gradient-spin-echo (OGSE) sequence ( $\leq 100\text{Hz}$ ) and accurately estimated fiber radius in an anisotropic fiber phantom on the Connectome 2.0 human scanner, demonstrating the potential of in vivo microstructural imaging using OGSE.

## Abstract Body (750 words)

### Introduction (119 words)

Diffusion time/frequency-dependence offers a direct probe to tissue microstructure at diffusion length  $\propto\sqrt{t}$ . For pulsed-gradient-spin-echo (PGSE) sequence, the shortest diffusion time is limited by the width of refocusing RF pulse<sup>2</sup>, leading to a minimum diffusion time  $\sim 10$ ms on human scanners. On the other hand, oscillating-gradient-spin-echo (OGSE) sequence offers a much shorter effective time scale<sup>3,4</sup>; in surface-to-volume ratio (SVR) limit, the OGSE has an effective diffusion time  $t_{\text{OGSE}} = (9/64) \cdot (2\pi/\omega)$ <sup>1,5</sup>, yielding a time scale  $\sim 1.4$ ms at 100Hz. Here we performed diffusion measurements using cosine-OGSE of varying frequency=30-100Hz in an anisotropic solid-fiber phantom<sup>6,7</sup> on Connectome 2.0 scanner<sup>8</sup> ( $G_{\text{max}}=500$ mT/m,  $SR_{\text{max}}=600$ T/m/s) and accurately estimated the fiber radius through the frequency-dependent diffusivity in SVR limit of OGSE, demonstrating the potential of in vivo microstructural imaging using OGSE<sup>9-11</sup>.

### Theory (285 words)

**SVR limit in OGSE.** At very short diffusion time, diffusion is restricted around barriers within a layer of diffusion length  $\propto\sqrt{t}$ , leading to a diffusivity decrease with  $SVR \cdot \sqrt{t}$ <sup>12</sup>. However, identifying this  $\sqrt{t}$ -term requires very short, making it almost impossible to observe using PGSE due to very low diffusion weighting (b-value) at short, making it almost impossible to observe using PGSE due to very low diffusion weighting (b-value) at short<sup>1,5,13</sup>. Therefore, this SVR regime is best observed using OGSE. The dispersive diffusivity  $\{\mathcal{D}\}(\omega)$  at frequency  $\omega$  in this limit is<sup>1,13</sup>

$$\{\mathcal{D}\}(\omega) \simeq D_0 \left(1 - \text{SVR} \cdot \frac{e^{i\pi/4}}{d} \cdot \sqrt{\frac{D_0}{\omega}}\right) \quad (1)$$

with intrinsic diffusivity  $D_0$ , and dimensionality  $d$ . Under Gaussian phase approximation, normalized diffusion signal is given by

$$-\ln \frac{S}{S_0} = \int \frac{d\omega}{2\pi} \{\mathcal{D}\}(\omega) |q(\omega)|^2 \quad (2)$$

where  $q(\omega)$  is the Fourier transform of diffusion wave vector  $q(t)$  (Figure 1). For an ideal cosine-OGSE waveform, the power spectrum  $|q(\omega)|^2$  has two delta-function peaks at  $\omega$  and  $-\omega$ , leading to an apparent diffusivity

$$D_{\text{OGSE}}(\omega) \equiv -\frac{1}{b} \ln \frac{S}{S_0} = \text{Re}\{\{\mathcal{D}\}(\omega)\} \quad (3)$$

with  $\{\mathcal{D}\}(\omega)$  in Eq.(1). Performing a linear fit of  $1/\sqrt{\omega}$  to

apparent diffusivity measured by OGSE yields an estimate of SVR in Eqs. (1) and (3).

**Fiber radius estimation.** Considering a phantom composed of randomly-packed parallel solid-fibers submersed in water, the SVR of extra-fiber space transverse to fibers is<sup>5</sup>

$$\text{SVR} = \frac{2}{R} \frac{f}{1-f}$$

or

$$R = \frac{2}{\text{SVR}} \frac{f}{1-f} \quad (4)$$

where the solid-fiber volume fraction  $f$  is estimated through  $b=0$  image signals  $S_0$  in the fiber bundle and free water area<sup>5</sup> (Figure 3)

$$f = 1 - \frac{S_0(\text{fiber bundle})}{S_0(\text{free water})} \quad (5)$$

**Fiber radius correction curve.** To account for the trapezoidal shape in the actual OGSE waveform with finite oscillation number  $N$  (Figures 1-2)<sup>1</sup>, we numerically simulated the diffusivity frequency-dependence of OGSE by substituting Eq.(1) and actual gradient waveform  $q(t)$  into Eq.(2). We fitted the SVR limit (Eq.(3)) to simulated frequency-dependent diffusivity to estimate the SVR. By comparing the ground truth and fitted value of SVR, we created a correction curve for SVR and fiber radius estimate (Eq.(4)) (Figure 4A).

## Methods (215 words)

**Fiber phantom.** We used a phantom composed of highly aligned Dyneema<sup>®</sup> solid fibers submersed in water, with a fiber radius  $R = 8.5 \pm 1.4 \mu\text{m}$ <sup>6,7</sup> (Figure 3A).

**MRI.** We performed diffusion MRI measurements in the fiber phantom by using an OGSE sequence featuring a trapezoidal-cosine gradient waveform (Figure 1). We varied OGSE frequency=30-100Hz with the cycle number  $N=1$  or 2 over each side of the refocusing RF pulse. Other parameters:  $b\text{-value}=[400, 850] \text{ s/mm}^2$  (20 directions/b-shell),  $\text{TR/TE}=2100/105\text{ms}$ . More details are in Figure 2.

**Image Processing.** dMRI data were processed based on DESIGNER pipeline<sup>14</sup> (Figure 3B). At each frequency, we performed diffusion kurtosis imaging fitting<sup>15</sup> and estimated radial diffusivity (RD) transverse to the fiber bundle. The masks of fiber bundle and free water area were manually segmented. We computed the median of RD in the fiber bundle at each frequency and averaged  $b=0$  signals in the fiber bundle and free water to estimate the solid-fiber volume fraction (Eq.(5)).

**Model fitting.** Empirically, to estimate SVR, the frequency-dependent RD was fitted to

$$D_{\text{OGSE}}(\omega) = D_0 \left( 1 - \text{SVR} \right) \cdot \frac{1}{\sqrt{2}} \cdot \sqrt{\frac{D_0}{\omega}}$$

$$D_0 \left( \frac{\alpha}{\omega} \right)^2 \quad (6)$$

where a higher order  $1/\omega$ -term accounts for surface relaxation of Dyneema fibers<sup>6,7</sup>,  $d=2$  transverse to fibers, and  $D_0$  is derived from the intercept of the fitted equation (3). Then we estimated the fiber radius from SVR value (Eq.(4)) and correct radius estimates using the correction curve (Figure 4A).

## Results (59 words)

In simulations of realistic OGSE waveform (Figure 4A, left), RD linearly decreased with  $1/\sqrt{\omega}$ . By using a simple linear correction curve for fiber radius estimate (Figure 4A, right), the estimation error is <5% when ground truth radius >0.4 $\mu$ m.

In phantom scan, RD decreased non-linearly due to an additional  $1/\omega$ -term (Eq.(6)) with an estimated radius =  $8.91 \pm 1.93 \mu\text{m}$ , consistent with the Dyneema fiber radius =  $8.5 \pm 1.3 \mu\text{m}$  (error = 4.8%).

## Discussion and Conclusion (65 words)

We measured frequency-dependent diffusivity using OGSE up to 100Hz and accurately estimated fiber radius in an anisotropic fiber phantom on the Connectome 2.0 human scanner, whose high-gradient performance enabled us to achieve high b-values over a wide frequency range while maintaining a reasonable SNR.

We conducted preliminary in-vivo experiments and observed that diffusivity increases and kurtosis decreases with frequency, consistent with previous results<sup>10,11</sup> (Figure 5).

## Acknowledgement

We would like to thank Dr. Dmitry S Novikov and Dr. Els Fieremans for the fruitful discussion and their generosity in sharing the Dyneema fiber phantom for scans. This study is supported by the National Institute of Health under the award numbers: DP5OD031854, R01NS118187, P41EB015896, P41EB030006, U01EB026996, U24NS137077.

## Reference

1. Novikov DS, Fieremans E, Jespersen SN, Kiselev VG. Quantifying brain microstructure with diffusion MRI: Theory and parameter estimation. *NMR Biomed.* 2019;32(4):e3998.
2. Stejskal EO, Tanner JE. Spin diffusion measurements: spin echoes in the presence of a time - dependent field gradient. *J Chem Phys.* 1965;42(1):288-292.
3. Gross B, Kosfeld R. Anwendung der spin-echo-methode der messung der selbstdiffusion.

Messtechnik. 1969;77:171-177.

4. Tanner JE. Self diffusion of water in frog muscle. *Biophys J*. 1979;28(1):107-116.
5. Lemberskiy G, Baete SH, Cloos MA, et al. Validation of surface-to-volume ratio measurements derived from oscillating gradient spin echo on a clinical scanner using anisotropic fiber phantoms. *NMR Biomed*. 2017;30(5):e3708.
6. Fieremans E, De Deene Y, Delpitte S, Özdemir MS, D' Asseler Y, Vlassenbroeck J, et al. Simulation and experimental verification of the diffusion in an anisotropic fiber phantom. *J Magn Reson*. 2008;190(2):189-199.
7. Burcaw LM, Fieremans E, Novikov DS. Mesoscopic structure of neuronal tracts from time-dependent diffusion. *NeuroImage*. 2015;114:18-37.
8. Huang SY, Witzel T, Keil B, et al. Connectome 2.0: Developing the next-generation ultra-high gradient strength human MRI scanner for bridging studies of the micro-, meso- and macro-connectome. *NeuroImage*. 2021;243:118530.
9. Xu J. Probing neural tissues at small scales: Recent progress of oscillating gradient spin echo (OGSE) neuroimaging in humans. *J Neurosci Methods*. 2021;349:109024.
10. Dai E, Zhu A, Yang GK, et al. Frequency-dependent diffusion kurtosis imaging in the human brain using an oscillating gradient spin echo sequence and a high-performance head-only gradient. *NeuroImage*. 2023;279:120328.
11. Hamilton J, Xu K, Geremia N, et al. Robust frequency-dependent diffusional kurtosis computation using an efficient direction scheme, axisymmetric modelling, and spatial regularization. *Imaging Neurosci*. 2024;2:1-22.
12. Mitra PP, Sen PN, Schwartz LM. Short-time behavior of the diffusion coefficient as a geometrical probe of porous media. *Phys Rev B*. 1993;47(14):8565.
13. Novikov DS, Kiselev VG. Surface-to-volume ratio with oscillating gradients. *J Magn Reson*. 2011;210(1):141-145.
14. Ades-Aron B, Veraart J, Kochunov P, et al. Evaluation of the accuracy and precision of the diffusion parameter EStImation with Gibbs and NoisE removal pipeline. *NeuroImage*. 2018;183:532-543.

## Figures and caption

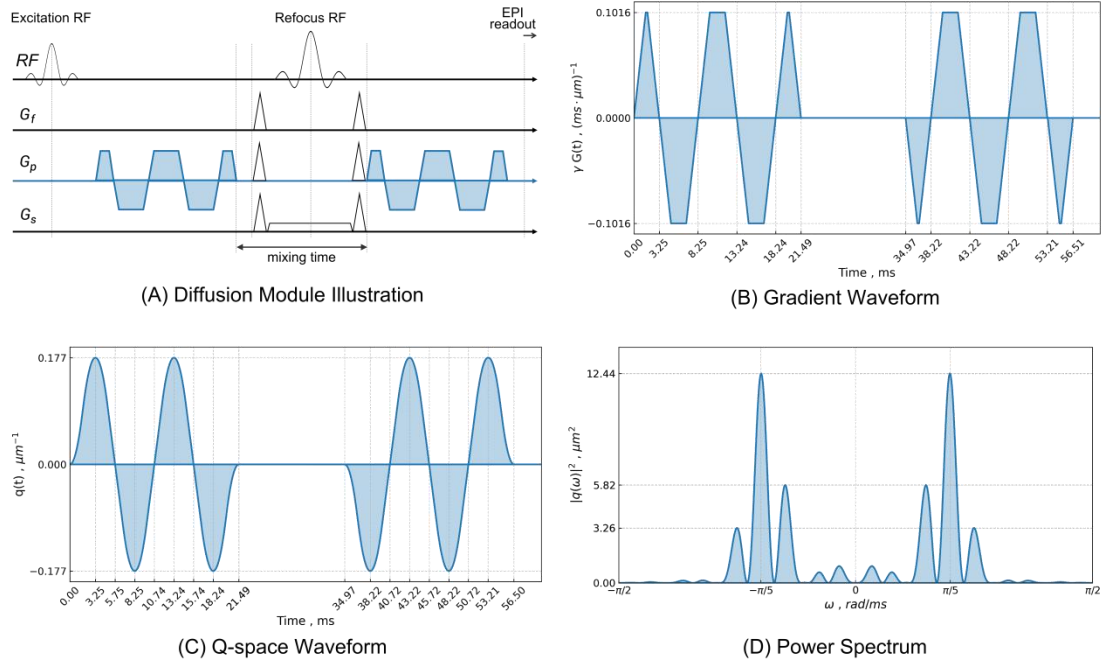
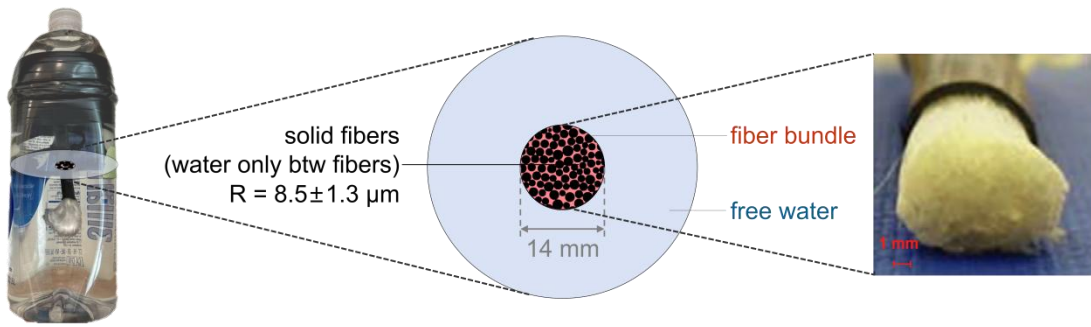


**Fig 1.** (A) Diffusion module in OGSE sequence, with refocusing RF pulse and field gradient in frequency encoding ( $G_f$ ), phase encoding ( $G_p$ ), and slice selection ( $G_s$ ) directions, and diffusion gradient applied in the  $G_p$  direction as an example. (B) Diffusion gradient waveform  $\gamma G(t)$  of OGSE sequence at frequency = 100 Hz with 2 cycles over each side of refocusing RF pulse. The mixing time in the middle accommodates the refocusing RF pulse. (C) Q-space waveform  $q(t)$ , defined as the integration of  $\gamma G(t)$  over time. (D) Power Spectrum  $|q(\omega)|^2$ , defined as the square of the Fourier transform of  $q(t)$ .

Parameter	Value(s)							
Maximum gradient $G_{\max}$ (mT/m)	400							
Maximum slew rate $SR_{\max}$ (T/m/s)	250							
FOV <sub>read</sub> (mm)	120							
Slice Thickness (mm)	5							
In-Plane Resolution (mm <sup>2</sup> )	1.5 × 1.5							
TR/TE (ms)	2100 / 105							
Diffusion Encoding	1 b = 0 image per b-value, 20 directions per b-value, b = 400, 850 s/mm <sup>2</sup>							
Frequency (Hz)	30	40	50	55	75	90	100	
Number of Cycle in Each Side	1	1	1	1	2	2	2	
Mixing Time (ms)	15.07	10.90	8.40	25.67	18.40	15.07	13.40	

**Fig 2.** Diffusion MRI Protocol in phantom scan. The gradient strength and slew rate of OGSE are set conservatively to avoid the hardware damage on Connectome 2.0 scanner. Advanced protocol will be tested in the future. The frequency of OGSE varied from 30 to 100 Hz, with as many cycle numbers as possible for the given TE. The optimal mixing time is adaptively calculated to minimize side lobes in the power spectrum of gradient waveform. FOV<sub>read</sub>=field of view in readout direction, TR=repetition time, TE=echo time

(A) Phantom Material (*Burcaw et al., NeuroImage 2015*)



(B) Processing Pipeline

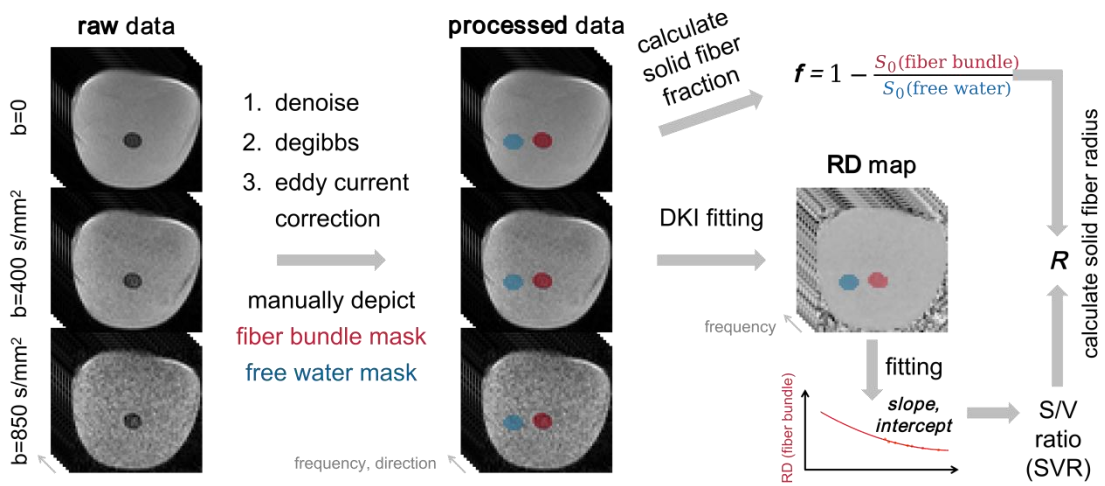


**Fig 3.** (A) Solid fiber phantom which has a fiber bundle composed of densely packed solid Dynemma® fibers (water-free inside) submersed in water, mimicking extra-axonal space in brain white matter. (B) Raw dMRI data at various frequencies are processed using DESIGNER pipeline. Masks for fiber bundle and free water areas are manually drawn. Volume fraction  $f$  of solid fibers is calculated using  $b=0$  signals. DKI fitting yields RD maps at each  $\omega$ . Fitting of RD in the fiber bundle v.s.  $1/\sqrt{\omega}$  yields the SVR value. Using SVR,  $f$  and correction curve in Fig. 4A, the fiber radius  $R$  is estimated.

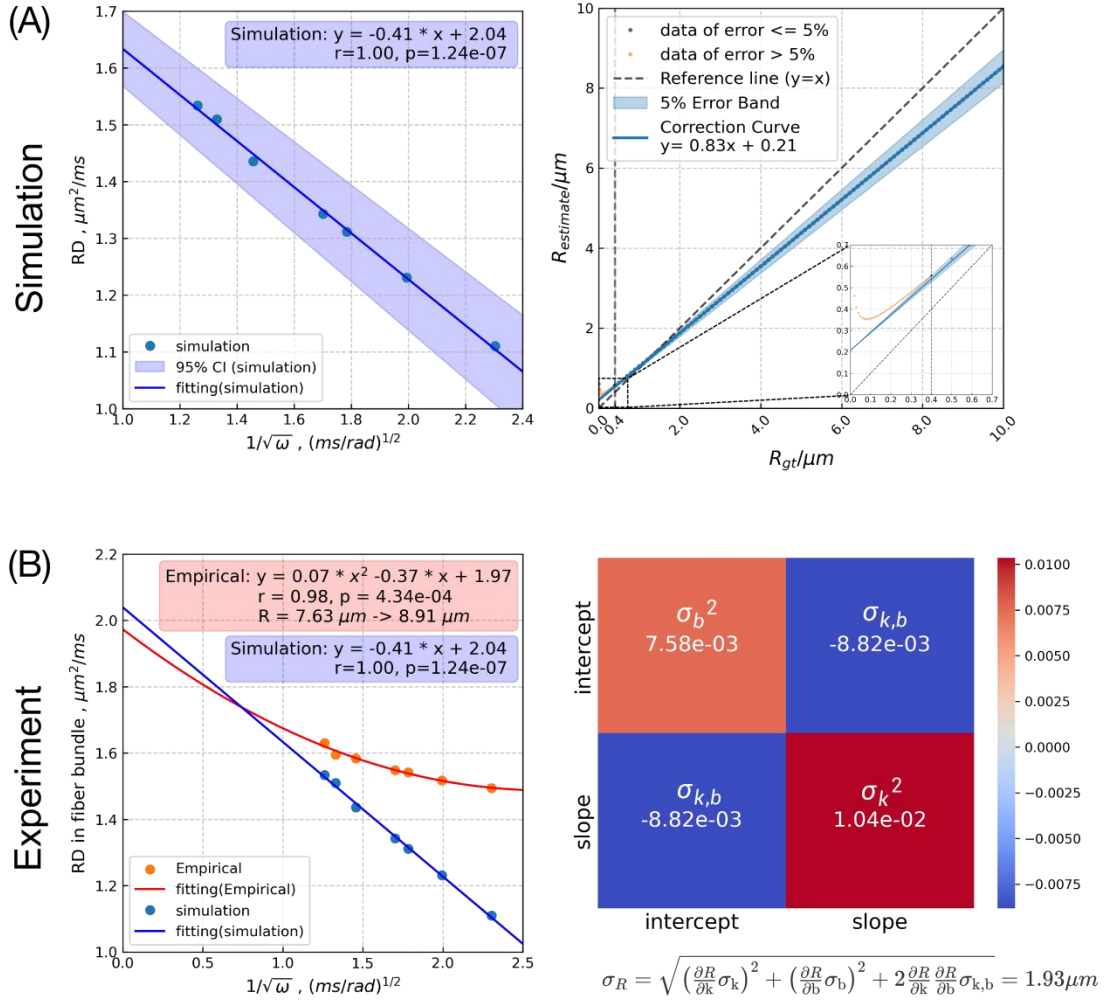


**Fig 4.** (A) Left: Simulations at fiber radius  $R=8.5 \mu\text{m}$  show strong RD vs.  $1/\sqrt{\omega}$  linearity. Right: Correction curve is created for imperfect sequence by estimating  $R$  values with various ground truth  $R$  values in simulation. After correction, error  $< 5\%$  for ground truth  $R > 0.4 \mu\text{m}$ . (B) Left: Phantom experiment (red) and simulation at ground truth  $R=8.5 \mu\text{m}$  (blue) are compared; experimental data show an additional  $1/\omega$  term due to surface relaxation. Using right panel in A, estimated  $R=7.63 \mu\text{m}$  is corrected to  $R=8.91 \mu\text{m}$  (error=4.8%). Right: From the fit's variance matrix,  $\sigma(R)=1.93 \mu\text{m}$  is calculated.

### (A) Protocol

Parameter	Value(s)		
Maximum gradient $G_{\max}$ (mT/m)	500		
Maximum slew rate $SR_{\max}$ (T/m/s)	300		
In-Plane Resolution (mm <sup>2</sup> )	$2 \times 2$		
Slice Thickness (mm)	2		
TR/TE (ms)	7600 / 110		
Diffusion Encoding	1 b = 0 image per b-value, 20 directions per b-value, b = 1000, 2000 s/mm <sup>2</sup>		
Frequency (Hz)	30	60	90
Number of Cycle in Each Side	1	2	3
Mixing Time (ms)	10		
Total Waveform Duration (ms)	80		
Accelerating Parameters	GRAPPA = 2, Partial Fourier = 6/8, SMS = 2		

### (B) Results

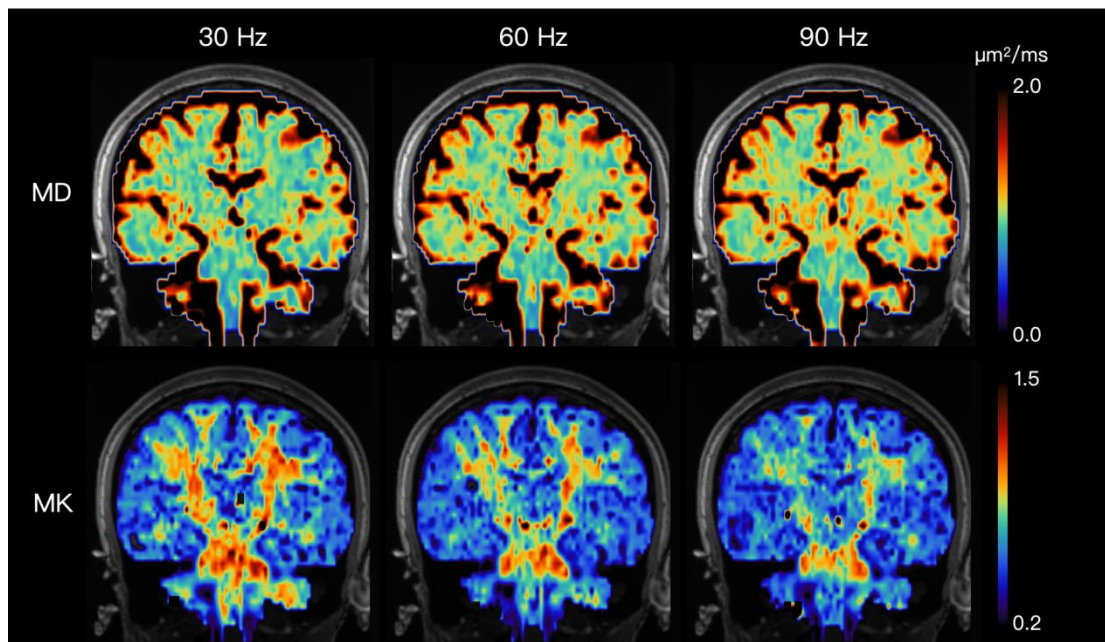


**Fig 5. In-vivo Experiment. (A) Protocol in human scan. (B) Results for human scan.** The images exhibit reasonable SNR, enabling detailed subsequent analysis. DKI fitting reveals that diffusivity increases with frequency and kurtosis decreases with frequency, which is consistent with previous findings. Future experiments aim to extract microstructural metrics from frequency dependence, striving to use OGSE for in vivo brain microstructure modeling.